ACS OMEGA

Open Access

http://pubs.acs.org/journal/acsodf

Article

Design, Synthesis, and Evaluation of New Pyrazolines As Small Molecule Inhibitors of Acetylcholinesterase

Mehlika Dilek Altıntop, Begüm Nurpelin Sağlık Özkan, and Ahmet Özdemir*

Cite This: *ACS Omega* 2024, 9, 31401−31409

Read Online

ACCESS | Metrics & More | Article Recommendations | Supporting Information

ABSTRACT: In pursuit of identifying small molecule inhibitors of acetylcholinesterase (AChE), the synthesis of new 2-pyrazolines was performed efficiently. A modified spectrophotometric method was used to examine their inhibitory effects on AChE as well as butyrylcholinesterase. Four compounds (**2a**, **2g**, **2j**, and **2l**) were identified as selective AChE inhibitors. Molecular docking studies were conducted to explore their potential interactions with the active site of AChE (PDB code: 4EY7). 1-(3-Nitrophenyl)-3-(thiophen-3-yl)-5-[4-(4-morpholinyl)phenyl]-2-pyrazoline (**2l**) exerted significant AChE inhibitory action with an IC_{50} value of 0.040 μM close to donepezil (IC_{50} = 0.021 μM). In addition to $\pi-\pi$ interactions with Tyr341, Tyr124, and Trp86 residues, compound **2l** was also capable of forming two hydrogen bonds and a salt bridge at the active site of AChE thanks to its nitro group at the *meta* position of the phenyl moiety linked to the N^1 position of the pyrazoline scaffold. The higher inhibitory effect of compound **2l** on AChE when compared to other compounds in this series might be explained by these additional interactions. Based on the *in vitro* parallel artificial membrane permeability assay, compound **2l** was found to have high blood−brain barrier permeability. *In vitro* and *in silico* studies suggest that compound **2l** is a potent inhibitor of AChE, which is an important target for neurodegenerative disorders, particularly Alzheimer's disease.

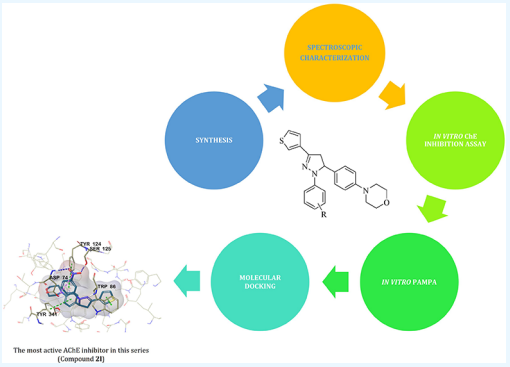

1. INTRODUCTION

Alzheimer's disease (AD) is the most common type of dementia, which is reported as a public health priority by the World Health Organization (WHO). The disease is predicted to affect over 100 million people worldwide by 2050, posing a serious threat to global healthcare systems in the future.[1−3]

AD is a devastating neurodegenerative disorder in the elderly with insidious onset and chronic progress. The severity of AD is reported to be closely associated with a progressive disruption of the cholinergic system, which is crucial for neuronal plasticity as well as mechanisms of learning and memory. The progressive loss of cholinergic neurons contributes to age-related memory loss and cognitive impairments that characterize AD, accompanied by other alterations, such as brain atrophy, resulting from cell death and inflammation.[1−4]

The cholinergic system is regulated by the acetylcholinesterase (AChE), which rapidly hydrolyzes the acetylcholine (ACh) in the central and peripheral nervous systems and halts impulse transmission at cholinergic synapses,[3] and therefore, the inhibition of the AChE enzyme is still a viable strategy in the fight against AD. There are currently three anti-AD drugs (Figure 1) that exert their action by inhibiting the AChE enzyme. Donepezil and galantamine are rapid-acting AChE inhibitors, whereas rivastigmine is a slow-acting inhibitor of both AChE and butyrylcholinesterase (BuChE). These agents raise ACh levels and thus provide symptomatic amelioration. However, none of them stops the progressive loss of neurons.[3−7]

Even after more than a century, no drug has been discovered to cure AD and reverse AD-related neurodegeneration since the development of anti-AD agents is challenging because of the unclear and complicated pathogenesis of AD. As a result, targeted anti-AD drug discovery is still a hot topic to which tremendous efforts are devoted.[1−11]

The unique features of pyrazolines (particularly 2-pyrazolines), allowing them to properly interact with pivotal residues of crucial biological targets, make the pyrazoline a privileged scaffold for the discovery of small molecules in the management of several diseases (e.g., neurodegenerative disorders, inflammatory diseases, cancer).[12−19] The pyrazoline ring is also used as a distinguished bioisostere of heterocycles such as imidazole, triazole, tetrazole, thiazole, oxazole, and isoxazole rings due to the fact that it is capable of modulating favorably physicochemical and biological profiles of ligands.[12] Several studies have highlighted that pyrazolines exert marked

Received: December 29, 2023
Revised: April 15, 2024
Accepted: April 23, 2024
Published: July 13, 2024

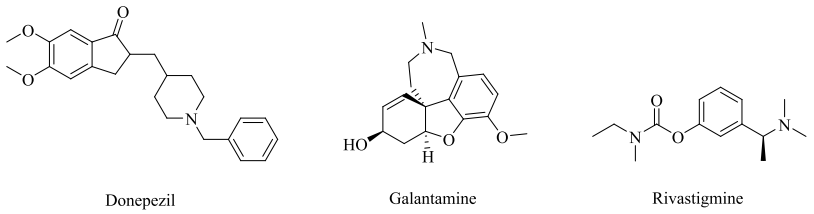

Figure 1. Currently available AChE inhibitors for AD therapy.

inhibitory activity against a plethora of enzymes related to the pathogenesis of AD, particularly AChE.[20−26]

The thiophene scaffold serves as an intriguing isostere of the benzene ring to improve the pharmacodynamic and pharmacokinetic properties of a drug.[27,28] Thiophenes have been reported to show inhibitory effects on AD-related targets including AChE and so on.[27−31]

In continuation of our previous work on the pyrazoline-based AChE inhibitors (Figure 2),[25] we designed a new class

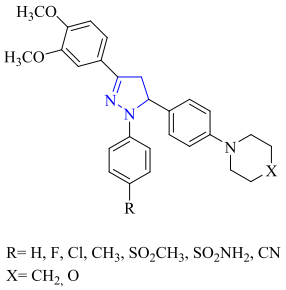

Figure 2. Pyrazoline-based small molecules that inspired this work.[25]

of AChE inhibitors by means of the molecular hybridization of the pyrazoline scaffold with the thiophene ring based on the publications describing the significant inhibition of AChE caused by pyrazolines[20−26] and thiophenes.[27−31] In this context, the synthesis of the designed pyrazolines was performed efficiently. *In vitro* studies were conducted for evaluating their inhibitory effects on AChE and BuChE. The most potent AChE inhibitors were examined for their ability to cross the blood−brain barrier (BBB). To shed light on the interactions of the most potent compounds with the active site of AChE, molecular docking studies were carried out.

2. RESULTS AND DISCUSSION

2.1. Chemistry. A two-step synthetic route was used to obtain the hitherto unreported pyrazoline-based small molecules (**2a−l**) (Scheme 1). The Claisen−Schmidt condensation of 3-acetylthiophene with 4-(4-morpholinyl)-benzaldehyde yielded 3-(4-morpholinophenyl)-1-(thiophen-3-yl)prop-2-en-1-one (**1**), which underwent a subsequent ring closure with appropriate arylhydrazine hydrochloride affording compounds **2a−l**.

Scheme 1. Synthesis of Compounds 2a−l[a]

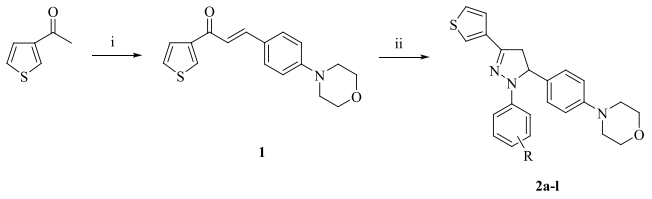

[a]Reagents and conditions: (i) 4-(4-morpholinyl)benzaldehyde, 40% sodium hydroxide solution, ethanol, rt, 24 h; (ii) arylhydrazine hydrochloride, ethanol, reflux, 16 h.

The structures of compounds **2a−l** were verified by infrared (IR), nuclear magnetic resonance (NMR, ^{1}H and ^{13}C), and high-resolution mass spectrometry (HRMS) data. The C═O stretching band was observed at 1643.35 cm^{-1} in the IR spectrum of compound **1**, the α,β-unsaturated ketone used as the starting compound for the preparation of compounds **2a−l**. The absence of this band in the IR spectra of compounds **2a−l** revealed that the cyclization reaction occurred efficiently for the formation of the pyrazoline ring. The ^{1}H NMR spectra of compounds **2a−l** confirmed the presence of the ABX pattern (Figure 3), which is a characteristic feature of the ^{1}H NMR

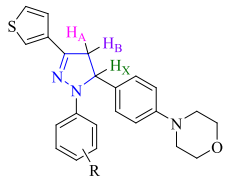

Figure 3. ABX pattern of the 2-pyrazoline ring for compounds **2a−l**.

spectra for the 2-pyrazoline core.[34] In their ^{1}H NMR spectra, the H_A, H_B, and H_X protons of the pyrazoline ring gave rise to the doublet of doublets at 3.00−3.14, 3.78−3.90 and 5.21−5.51 ppm, respectively, with J_{AB} = 16.15−17.65 Hz, J_{BA} = 17.25−17.65 Hz, J_{AX} = 4.70−7.20 Hz, and J_{BX} = 11.80−12.05 Hz. In the ^{13}C NMR spectra of compounds **2a−l**, the signals were observed in the region 150.66−150.91, 44.28−44.65, and 61.89−64.00 ppm corresponding to the C3, C4, and C5 carbons of the pyrazoline skeleton, respectively.

2.2. AChE and BuChE Inhibitory Activity. All compounds were subjected to a modified spectrophotometric method described by Ellman et al.[32] to determine their inhibitory effects on AChE and BuChE. As presented in Table 1, the tested compounds did not cause any inhibitory activity against BuChE (the IC_{50} values of the obtained compounds were higher than 1000 μM). It was observed that the synthesized compounds showed selective AChE enzyme inhibition.

Among the tested compounds, compounds **2a**, **2g**, **2j**, and **2l** exerted marked AChE inhibition with IC_{50} values of 0.107, 0.122, 0.062, and 0.040 μM compared to donepezil (IC_{50} = 0.021 μM).

Due to their strong inhibitory effects on AChE (Table 1), the inhibition% caused by each compound was evaluated at concentrations ranging from 10^{-3} to 10^{-9} M (Table 2). It can be concluded that the AChE inhibitory potency depends on the substituent at the *para*/*meta* position of the phenyl moiety attached to the N^1 position of the pyrazoline ring. The nitro

https://doi.org/10.1021/acsomega.3c10490
ACS Omega 2024, 9, 31401−31409

Table 1. Inhibitory Effects of the Synthesized Compounds and the Positive Controls on AChE and BuChE[a]

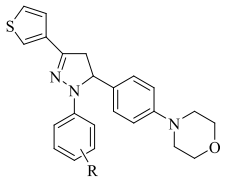

		human AChE			human BuChE		
		inhibition %			inhibition%		
compound	R	10^{-3} M	10^{-4} M	IC_{50} (μM)	10^{-3} M	10^{-4} M	IC_{50} (μM)
1		78.35 ± 2.10	41.06 ± 1.87	>100	46.56 ± 0.92	21.34 ± 0.84	>1000
2a	H	91.41 ± 2.46	88.56 ± 2.06	0.107 ± 0.0048	31.14 ± 0.84	18.15 ± 0.76	>1000
2b	4-SO_2CH_3	40.59 ± 1.76	23.13 ± 0.95	>1000	26.45 ± 0.75	15.06 ± 0.78	>1000
2c	4-CH_3	73.64 ± 2.06	38.67 ± 1.34	>100	29.32 ± 0.99	20.62 ± 0.82	>1000
2d	4-OCH_3	84.55 ± 2.36	44.18 ± 1.24	>100	33.13 ± 0.99	21.05 ± 0.86	>1000
2e	4-CN	81.22 ± 1.91	47.56 ± 1.85	>100	38.92 ± 1.22	23.43 ± 1.06	>1000
2f	4-F	71.44 ± 2.46	45.35 ± 1.99	>100	31.53 ± 1.15	21.92 ± 0.89	>1000
2g	4-Cl	90.72 ± 1.15	86.63 ± 2.56	0.122 ± 0.0051	25.03 ± 0.96	20.75 ± 0.93	>1000
2h	4-Br	46.46 ± 1.94	20.85 ± 0.83	>1000	40.76 ± 1.94	26.16 ± 1.25	>1000
2i	3-F	68.32 ± 2.15	37.64 ± 1.51	>100	36.21 ± 1.42	27.45 ± 1.38	>1000
2j	3-Cl	93.13 ± 2.85	89.49 ± 1.85	0.062 ± 0.0030	34.33 ± 1.55	24.87 ± 0.97	>1000
2k	3-Br	45.82 ± 1.72	30.34 ± 1.03	>1000	28.97 ± 1.09	17.59 ± 0.81	>1000
2l	3-NO_2	95.35 ± 2.03	91.65 ± 1.92	0.040 ± 0.0019	30.46 ± 0.97	19.29 ± 0.82	>1000
donepezil		99.16 ± 1.30	97.40 ± 1.26	0.021 ± 0.0009			
tacrine					99.83 ± 1.38	98.65 ± 1.40	0.006 ± 0.0002

[a]The test results were expressed as means of quartet assays.

Table 2. Inhibition% and IC_{50} Values of the most Potent Inhibitors and Donepezil for AChE[a]

	human AChE inhibition%							
compound	10^{-3} M	10^{-4} M	10^{-5} M	10^{-6} M	10^{-7} M	10^{-8} M	10^{-9} M	IC_{50} (μM)
2a	91.41 ± 2.46	88.56 ± 2.06	84.75 ± 1.80	82.51 ± 1.91	49.68 ± 1.74	20.32 ± 0.99	14.65 ± 0.66	0.107 ± 0.0048
2g	90.72 ± 1.15	86.63 ± 2.56	82.42 ± 2.17	79.55 ± 1.57	47.91 ± 0.96	23.10 ± 1.06	15.64 ± 0.73	0.122 ± 0.0051
2j	93.13 ± 2.85	89.49 ± 1.85	80.23 ± 2.16	72.05 ± 1.78	60.79 ± 1.64	36.19 ± 0.98	18.97 ± 0.63	0.062 ± 0.0030
2l	95.35 ± 2.03	91.65 ± 1.92	82.57 ± 1.51	75.37 ± 1.03	64.56 ± 1.85	42.21 ± 1.52	19.33 ± 0.75	0.040 ± 0.0019
donepezil	99.16 ± 1.30	97.40 ± 1.26	93.58 ± 1.17	91.28 ± 1.07	76.98 ± 0.95	35.46 ± 0.45	18.41 ± 0.41	0.021 ± 0.0009

[a]The test results were expressed as means of quartet assays.

group at the *meta* position significantly enhanced AChE inhibitory activity. The chloro substitution, particularly at the *meta* position, led to a marked increase in AChE inhibition. The methylsulfonyl group at the *para* position and the bromo substituent at the *meta* and the *para* positions of the phenyl moiety dramatically diminished AChE inhibitory activity (Table 1).

2.3. *In Vitro* BBB Permeability Assay. To evaluate the BBB permeability of the effective derivatives (**2a**, **2g**, **2j**, and **2l**), *in vitro* parallel artificial membrane permeability assay (PAMPA) was applied. The obtained results are presented in Table 3. Compounds **2a** and **2l** were found to have high BBB permeability.

2.4. Molecular Docking Studies. Docking experiments were conducted on the crystal structure of AChE (PDB Code: 4EY7)[33] to ascertain the potential interactions of the most potent AChE inhibitors in this series (compounds **2a**, **2g**, **2j**, and **2l**) with the enzyme active site. The docking scores and docking poses of the related compounds, which express the binding affinities obtained as a result of the molecular docking process performed with the AChE enzyme crystal structure, are given in Table 4 and Figure 4, respectively. As can be seen from Table 4, compounds **2a**, **2g**, **2j**, and **2l** show close binding scores to the reference compound, donepezil. At this point, compound **2l** displays the closest binding affinity to donepezil with its binding scores (Docking score: −8.40 kcal/mol, Glide score: −8.40 kcal/mol, Glide emodel: −77.39 kcal/mol).

Table 3. Type of BBB Penetration of Compounds 2a, 2g, 2j, and 2l

classification	type of BBB permeation	compound	type of BBB permeation
CNS+	high BBB permeation P_e (10^{-6} cm s^{-1}) > 4.0	**2a**	**CNS+** high BBB permeation
		2l	**CNS+** high BBB permeation
CNS−	low BBB permeation P_e (10^{-6} cm s^{-1}) < 2.0		
CNS±	BBB permeation uncertain 2.0 < P_e (10^{-6} cm s^{-1}) < 4.0	**2g**	**CNS ±** uncertain BBB permeation
		2j	**CNS ±** uncertain BBB permeation

Figure 4 illustrates how the pyrazolines, particularly those that form direct interactions with the active site of the enzyme, have similar binding patterns. The interactions that all of these derivatives share may be summed up as follows. The thiophene at the third position of the pyrazoline ring formed a $\pi-\pi$

https://doi.org/10.1021/acsomega.3c10490
ACS Omega 2024, 9, 31401−31409

Table 4. Binding Affinities of Compounds 2a, 2g, 2j, 2l, and Donepezil to the AChE Enzyme

	binding affinities (kcal/mol)		
compound	docking score	glide score	glide emodel
2a	−7.06	−7.06	−64.62
2g	−7.51	−7.51	−69.10
2j	−7.45	−7.45	−69.86
2l	−8.40	−8.40	−77.39
donepezil	−9.87	−9.91	−85.51

interaction with the indole ring of Trp86 residue. This interaction with Trp86, an essential amino acid, revealed the location of the compounds inside the catalytic anionic site (CAS). It was observed that the 4-morpholinophenyl ring at the fifth position of the pyrazoline core formed $\pi-\pi$ interactions with the phenyl moieties of Tyr337, Tyr341, and Phe338. The last common $\pi-\pi$ interaction was observed between the *m*-/*p*-substituted phenyl ring at the first position of the pyrazoline ring and the phenyl moiety of Tyr124.

According to docking studies, the different interactions of these compounds with the active site of the AChE arise from the *p*- or *m*- substituents attached to the phenyl motif at the first position of the pyrazoline core. Because of the chlorine atom at the *m*- or the *p*- position of the phenyl ring, compounds **2g** and **2j** established halogen bonds with Tyr72 and Asp74 residues, respectively, as presented in Figure 4 (B, C). The *m*-nitro substituent of compound **2l** was capable of forming two hydrogen bonds with the amino group of Asp74 and the hydroxyl of Ser125. Also, it was detected that there was a salt bridge between this *m*-nitro group and Asp74 in Figure 4 (D, E). The more potent inhibitory potential of compound **2l** (IC_{50}= 0.040 μM) can be explained by the formation of these crucial bonds.

3. CONCLUSIONS

In conclusion, we designed a new series of small molecule AChE inhibitors via the molecular hybridization of the pyrazoline core with the thiophene ring. An efficient route was followed to synthesize new 2-pyrazoline derivatives, which were tested for their inhibitory effects on AChE as well as BuChE. The most potent AChE inhibitor was found as compound **2l** (IC_{50} = 0.040 μM) followed by compounds **2j** (IC_{50} = 0.062 μM), **2a** (IC_{50} = 0.107 μM), and **2g** (IC_{50} =

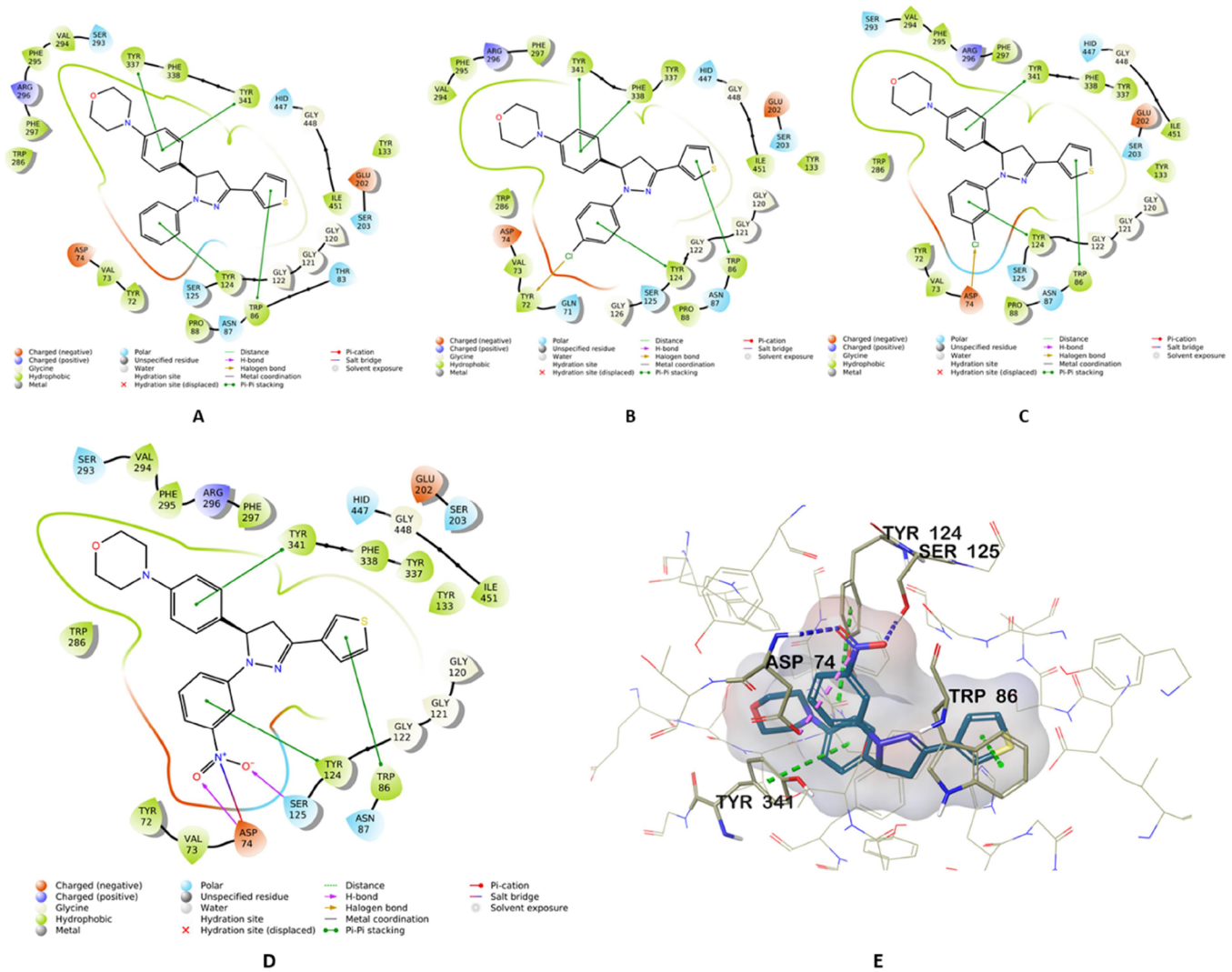

Figure 4. 2D interaction poses of compounds **2a** (A), **2g** (B), **2j** (C), and **2l** (D). The 3D interaction pose of compound **2l** (E) in the active site of AChE (PDB Code: 4EY7).

https://doi.org/10.1021/acsomega.3c10490
ACS Omega 2024, 9, 31401−31409

0.122 μM) when compared with donepezil (IC_{50} = 0.021 μM). On the other hand, the tested compounds did not cause any inhibitory effect on BuChE. *In vitro* and *in silico* data pointed out the importance of the nitro group at the *meta* position of the phenyl motif at the first position of the pyrazoline scaffold. The nitro group enables compound **2l** to form two hydrogen bonds and a salt bridge, enhancing its interactions with the AChE active site. The *in silico* studies supported the data obtained by *in vitro* experiments, showing that compound **2l** is the most effective AChE inhibitor in this series. Compound **2l** stands out as a strong inhibitor of AChE, a key target for neurodegenerative diseases, particularly AD. In the continuation of this research work, *in vivo* studies are needed to illuminate the potential of compound **2l** for the management of AD.

4. MATERIALS AND METHODS

4.1. Chemistry. All reagents were procured from commercial vendors and were used without further purification. The melting points (Mp) of the compounds were determined on an Electrothermal IA9200 digital melting point device (Staffordshire, UK) and are uncorrected. IR spectra were recorded on the IRPrestige-21 Fourier Transform Infrared spectrophotometer (Shimadzu, Tokyo, Japan) equipped with an attenuated total reflection accessory. ^{1}H and ^{13}C NMR spectra were recorded on the Bruker AVANCE NEO 500 MHz NMR spectrometer (Bruker, Rheinstetten, Germany). HRMS spectra were acquired from the LCMS-IT-TOF system (Shimadzu, Kyoto, Japan). Thin-layer chromatography was used to monitor the progress of the chemical reactions and examine the purity of the synthesized compounds.

4.2. General Procedure for the Synthesis of the Compounds. *4.2.1. 3-(4-Morpholinophenyl)-1-(thiophen-3-yl)prop-2-en-1-one (**1**).* A mixture of 3-acetylthiophene (0.02 mol), 4-(4-morpholinyl)benzaldehyde (0.02 mol), and 40% (w/v) aqueous sodium hydroxide (8 mL) in ethanol (40 mL) was stirred at room temperature (rt) for 24 h. Upon completion of the reaction, the reaction mixture was poured into crushed ice. The precipitated solid was filtered, washed with water, and dried. The product was crystallized from ethanol.[34,35]

Pale yellow powder. Yield: 75%; Mp 137−139 °C. IR ν_{max} (cm^{-1}): 3086.11, 2964.59, 2839.22, 1643.35, 1604.77, 1566.20, 1550.77, 1510.26, 1446.61, 1427.32, 1409.96, 1379.10, 1348.24, 1325.10, 1307.74, 1267.23, 1244.09, 1219.01, 1168.86, 1111.00, 1066.64, 1053.13, 1022.27, 991.41, 923.90, 883.40, 860.25, 790.81, 759.95, 736,81, 696.30, 638.44, 626.87, 609.51. ^{1}H NMR (500 MHz, DMSO-d_6) δ (ppm): 3.25 (t, J = 4.50, 5.00 Hz, 4H), 3.74 (t, J = 4.50, 5.00 Hz, 4H), 7.00 (d, J = 8.50 Hz, 2H), 7.65 (s, 2H), 7.67 (d, J = 2.00 Hz, 2H), 7.74 (d, J = 8.85 Hz, 2H), 8.75 (t, J = 2.00 Hz, 1H). ^{13}C NMR (125 MHz, DMSO-d_6) δ (ppm): 47.65 ($2CH_2$), 66.37 ($2CH_2$), 114.60 (2CH), 119.40 (CH), 125.21 (C), 127.64 (CH), 127.86 (CH), 130.88 (2CH), 133.80 (CH), 143.81 (C), 143.94 (CH), 153.04 (C), 183.32 (C). HRMS (ESI) (m/z): $[M + H]^+$ calcd for $C_{17}H_{17}NO_2S$: 300.1053, found: 300.1067.

*4.2.2. 1-Aryl-3-(3-thienyl)-5-[4-(4-morpholinyl)phenyl]-2-pyrazolines (**2a**−**l**).* A mixture of compound **1** (10.0 mmol) and arylhydrazine hydrochloride (15.0 mmol) was refluxed for 16 h in absolute ethanol (30 mL) to yield 2-pyrazolines. Then, the reaction mixture was poured into crushed ice. The precipitate was separated by filtration, washed with water, and crystallized from ethanol.[36,37]

*4.2.2.1. 1-Phenyl-3-(thiophen-3-yl)-5-[4-(4-morpholinyl)-phenyl]-2-pyrazoline (**2a**).* Pale yellow powder. Yield: 87%. Mp 179−181 °C. IR ν_{max} (cm^{-1}): 3093.82, 2966.52, 2918.30, 2891.30, 2856.58, 2819.93, 1612.49, 1595.13, 1571.99, 1514.12, 1496.76, 1450.47, 1425.40, 1379.10, 1352.10, 1300.02, 1284.59, 1261.45, 1234.44, 1292.01, 1176.58, 1153.43, 1120.64, 1068.56, 1053.13, 1028.06, 997.20, 923.90, 871.82, 840.96, 817.82, 773.46, 744,52, 692.44, 671.23, 634.58, 624.94, 574.79, 545.85. ^{1}H NMR (500 MHz, DMSO-d_6) δ (ppm): 3.03 (dd, J_{AB} = 16.15 Hz, J_{AX} = 6.10 Hz, 1H), 3.05 (t, J = 4.80, 4.75 Hz, 4H), 3.70 (t, J = 4.65, 4.95 Hz, 4H), 3.83 (dd, J_{BA} = 17.30 Hz, J_{BX} = 12.00 Hz, 1H), 5.33 (dd, J_{BX} = 11.95 Hz, J_{AX} = 6.10 Hz, 1H), 6.69 (t, J = 7.25 Hz, 1H), 6.89 (d, J = 8.80 Hz, 2H), 6.99 (d, J = 8.68 Hz, 2H), 7.12−7.15 (m, 4H), 7.58 (dd, J = 1.15, 5.05 Hz, 1H), 7.64 (dd, J = 2.90, 5.05 Hz, 1H), 7.70 (dd, J = 1.15, 2.85 Hz, 1H). ^{13}C NMR (125 MHz, DMSO-d_6) δ (ppm): 44.33 (CH_2), 48.78 ($2CH_2$), 62.86 (CH), 66.55 ($2CH_2$), 113.38 (2CH), 115.90 (2CH), 118.70 (CH), 124.63 (CH), 125.67 (CH), 127.02 (2CH), 127.76 (CH), 129.25 (2CH), 133.38 (C), 135.34 (C), 144.82 (C), 144.92 (C), 150.69 (C). HRMS (m/z): $[M + H]^+$ calcd for $C_{23}H_{23}N_3OS$: 390.1635. Found: 390.1639.

*4.2.2.2. 1-(4-Methylsulfonylphenyl)-3-(thiophen-3-yl)-5-[4-(4-morpholinyl)phenyl]-2-pyrazoline (**2b**).* Beige powder. Yield: 53%. Mp 130−132 °C. IR ν_{max} (cm^{-1}): 3099.61, 2958.80, 2920.23, 2850.79, 2821.86, 1610.56, 1589.34, 1504.48, 1446.61, 1421.54, 1373.32, 1317.38, 1294.24, 1259.52, 1234.44, 1190.08, 1136.07, 1118.71, 1089.78, 1051.20, 1001.06, 954.76, 925.83, 873.75, 823.60, 769.60, 719.45, 705.95, 636.51, 626.87, 569.00. ^{1}H NMR (500 MHz, DMSO-d_6) δ (ppm): 3.05 (t, J = 4.80, 4.90 Hz, 4H), 3.07 (s, 3H), 3.13 (dd, J_{AB} = 17.65 Hz, J_{AX} = 4.85 Hz, 1H), 3.69 (t, J = 4.60, 5.00 Hz, 4H), 3.90 (dd, J_{BA} = 17.60 Hz, J_{BX} = 11.90 Hz, 1H), 5.51 (dd, J_{BX} = 11.80 Hz, J_{AX} = 4.75 Hz, 1H), 6.90 (d, J = 8.85 Hz, 2H), 7.11 (d, J = 8.65 Hz, 4H), 7.61−7.68 (m, 4H), 7.84 (dd, J = 1.20, 2.80 Hz, 1H). ^{13}C NMR (125 MHz, DMSO-d_6) δ (ppm): 44.40 (CH_3), 44.65 (CH_2), 48.64 ($2CH_2$), 61.95 (CH), 66.53 ($2CH_2$), 112.50 (2CH), 115.60 (2CH), 125.79 (CH), 126.38 (CH), 126.89 (2CH), 128.07 (CH), 128.96 (2CH), 129.09 (C), 132.19 (C), 134.64 (C), 147.63 (C), 147.96 (C), 150.89 (C). HRMS (m/z): $[M + H]^+$ calcd for $C_{24}H_{25}N_3O_3S_2$: 468.1410. Found: 468.1418.

*4.2.2.3. 1-(4-Methylphenyl)-3-(thiophen-3-yl)-5-[4-(4-morpholinyl)phenyl]-2-pyrazoline (**2c**).* Off-white powder. Yield: 74%. Mp 171−173 °C. IR ν_{max} (cm^{-1}): 3080.32, 3030.17, 3008.95, 2958.80, 2914.44, 2856.58, 2821.86, 1612.49, 1568.13, 1512.19, 1446.61, 1377.17, 1348.24, 1303.88, 1288.45, 1261.45, 1234.44, 1186.22, 1120.64, 1091.71, 1070.49, 1049.28, 1029.99, 1010.70, 995.27, 929.69, 875.68, 840.96, 817.82, 804.32, 773.46, 731.02, 704.02, 646.15, 626.87, 607.58, 572.86, 551.64. ^{1}H NMR (500 MHz, DMSO-d_6) δ (ppm): 2.15 (s, 3H), 3.01 (dd, J_{AB} = 17.15 Hz, J_{AX} = 6.30 Hz, 1H), 3.05 (t, J = 4.80 Hz, 4H), 3.70 (t, J = 4.60, 4.95 Hz, 4H), 3.78 (dd, J_{BA} = 17.25 Hz, J_{BX} = 12.05 Hz, 1H), 5.28 (dd, J_{BX} = 11.90 Hz, J_{AX} = 6.30 Hz, 1H), 6.87−6.90 (m, 4H), 6.94 (d, J = 8.50 Hz, 2H), 7.11 (d, J = 8.70 Hz, 2H), 7.57 (dd, J = 1.10, 5.05 Hz, 1H), 7.62−7.66 (m, 2H). ^{13}C NMR (125 MHz, DMSO-d_6) δ (ppm): 20.57 (CH_3), 44.28 (CH_2), 48.79 ($2CH_2$), 63.16 (CH), 66.55 ($2CH_2$), 113.57 (2CH), 115.85 (2CH), 124.29 (CH), 125.64 (CH), 127.06 (2CH), 127.59 (C), 127.69 (CH), 129.68 (2CH), 133.43 (C), 135.45 (C), 142.87 (C), 144.30 (C), 150.66 (C). HRMS (m/z): $[M + H]^+$ calcd for $C_{24}H_{25}N_3OS$: 404.1791. Found: 404.1793.

https://doi.org/10.1021/acsomega.3c10490
ACS Omega 2024, 9, 31401−31409

*4.2.2.4. 1-(4-Methoxyphenyl)-3-(thiophen-3-yl)-5-[4-(4-morpholinyl)phenyl]-2-pyrazoline (**2d**).* Khaki powder. Yield: 64%. Mp 122−124 °C. IR ν_{max} (cm^{-1}): 3101.54, 3082.25, 3010.88, 2956.87, 2916.37, 2848.86, 2827.64, 1610.56, 1573.91, 1552.70, 1506.41, 1463.97, 1444.68, 1425.40, 1379.10, 1357.89, 1305.81, 1288.45, 1259.52, 1236.37, 1182.36, 1170.79, 1116.78, 1099.43, 1068.56, 1031.92, 989.48, 925.83, 877.75, 862.18, 840.96, 812.03, 800.46, 788.89, 769.60, 738.74, 704.02, 650.01, 634.58, 626.87, 607.58, 576.72, 561.29. ^{1}H NMR (500 MHz, DMSO-d_6) δ (ppm): 3.00 (dd, J_{AB} = 17.10 Hz, J_{AX} = 7.15 Hz, 1H), 3.05 (t, J = 4.75, 4.80 Hz, 4H), 3.64 (s, 3H), 3.70 (t, J = 4.55, 4.95 Hz, 4H), 3.75−3.80 (m, 1H), 5.21 (dd, J_{BX} = 11.80 Hz, J_{AX} = 7.20 Hz, 1H), 6.76 (d, J = 9.10 Hz, 2H), 6.91 (d, J = 8.75 Hz, 2H), 7.00 (d, J = 8.90 Hz, 1H), 7.14 (d, J = 8.70 Hz, 2H), 7.55 (dd, J = 1.05, 5.00 Hz, 1H), 7.61−7.67 (m, 2H), 7.73−7.75 (m, 1H). ^{13}C NMR (125 MHz, DMSO-d_6) δ (ppm): 44.40 (CH_2), 48.21 ($2CH_2$, d, J = 140.13 Hz), 55.64 (CH_3), 64.00 (CH), 66.47 ($2CH_2$, d, J = 22.73 Hz), 114.81 (2CH, d, J = 19.09 Hz), 115.83 (2CH), 119.40 (CH), 124.09 (CH), 125.41 (CH, d, J = 52.09 Hz), 127.22 (2CH), 127.65 (CH, d, J = 4.48 Hz), 130.89 (CH), 133.61 (C, d, J = 50.09 Hz), 135.51 (C), 139.59 (C), 144.12 (C), 150.68 (C), 152.99 (C, d, J = 14.16 Hz). HRMS (m/z): $[M + H]^+$ calcd for $C_{24}H_{25}N_3O_2S$: 420.1740. Found: 420.1746.

*4.2.2.5. 1-(4-Cyanophenyl)-3-(thiophen-3-yl)-5-[4-(4-morpholinyl)phenyl]-2-pyrazoline (**2e**).* Light yellow powder. Yield: 73%. Mp 195−197 °C. IR ν_{max} (cm^{-1}): 3091.89, 2958.80, 2914.44, 2895.15, 2850.79, 2216.21, 1600.92, 1519.91, 1510.26, 1446.68, 1373.32, 1334.74, 1305.81, 1284.59, 1257.59, 1240.23, 1211.30, 1193.94, 1172.72, 1120.64, 1095.57, 1072.42, 1053.13, 1008.77, 991.41, 923.90, 871.82, 840.96, 823.60, 808.17, 773.46, 729.09, 709.80, 692.44, 621.08, 582.50, 572.86, 542.00. ^{1}H NMR (500 MHz, DMSO-d_6) δ (ppm): 3.05 (t, J = 4.80, 4.90 Hz, 4H), 3.13 (dd, J_{AB} = 17.65 Hz, J_{AX} = 4.80 Hz, 1H), 3.69 (t, J = 4.60, 5.00 Hz, 4H), 3.89 (dd, J_{BA} = 17.65 Hz, J_{BX} = 11.90 Hz, 1H), 5.50 (dd, J_{BX} = 11.80 Hz, J_{AX} = 4.70 Hz, 1H), 6.89 (d, J = 8.85 Hz, 2H), 7.05 (d, J = 8.80 Hz, 2H), 7.09 (d, J = 8.75 Hz, 2H), 7.54 (d, J = 9.10 Hz, 2H), 7.61 (dd, J = 1.20, 5.05 Hz, 1H), 7.67 (dd, J = 2.85, 5.10 Hz, 1H), 7.83−7.84 (m, 1H). ^{13}C NMR (125 MHz, DMSO-d_6) δ (ppm): 44.39 (CH_2), 48.64 ($2CH_2$), 61.89 (CH), 66.52 ($2CH_2$), 98.95 (C), 113.14 (2CH), 115.95 (2CH), 120.55 (C), 125.77 (CH), 126.49 (CH), 126.86 (2CH), 128.08 (CH), 132.09 (C), 133.69 (2CH), 134.59 (C), 147.12 (C), 148.18 (C), 150.91 (C). HRMS (m/z): $[M + H]^+$ calcd for $C_{24}H_{22}N_4OS$: 415.1587. Found: 415.1594.

*4.2.2.6. 1-(4-Fluorophenyl)-3-(thiophen-3-yl)-5-[4-(4-morpholinyl)phenyl]-2-pyrazoline (**2f**).* Light yellow powder. Yield: 85%. Mp 182−184 °C. IR ν_{max} (cm^{-1}): 3093.82, 3074.53, 2962.66, 2902.87, 2862.36, 2825.72, 1614.42, 1581.63, 1514.12, 1502.55, 1462.04, 1450.47, 1438.90, 1425.40, 1377.17, 1359.82, 1340.53, 1298.09, 1261.45, 1232.51, 1213.23, 1188.15, 1153.43, 1118.71, 1103.28, 1087.85, 1068.56, 1051.20, 1028.06, 1008.77, 993.34, 933.55, 923.90, 867.97, 840.96, 808.17, 796.60, 732.95, 709.80, 644.22, 628.79, 601.79, 578.64, 547.78. ^{1}H NMR (500 MHz, DMSO-d_6) δ (ppm): 3.01−3.06 (m, 5H), 3.70 (t, J = 4.60, 4.95 Hz, 4H), 3.81 (dd, J_{BA} = 17.30 Hz, J_{BX} = 12.00 Hz, 1H), 5.29 (dd, J_{BX} = 11.85 Hz, J_{AX} = 6.50 Hz, 1H), 6.89 (d, J = 8.80 Hz, 2H), 6.95−7.01 (m, 4H), 7.13 (d, J = 8.75 Hz, 2H), 7.57 (dd, J = 1.15, 5.05 Hz, 1H), 7.63−7.64 (m, 1H), 7.69−7.70 (m, 1H). ^{13}C NMR (125 MHz, DMSO-d_6) δ (ppm): 44.50 (CH_2), 48.72 ($2CH_2$), 63.45 (CH), 66.55 ($2CH_2$), 114.53 (d, J = 7.25 Hz, 2CH), 115.68 (CH), 115.87 (2CH), 124.73 (CH), 125.65 (CH), 127.12 (2CH), 127.78 (2CH), 133.04 (C), 135.24 (C), 141.91 (C), 145.07 (C), 150.75 (C), 155.25 and 157.11 (2s, C). HRMS (m/z): $[M + H]^+$ calcd for $C_{23}H_{22}FN_3OS$: 408.1540. Found: 408.1540.

*4.2.2.7. 1-(4-Chlorophenyl)-3-(thiophen-3-yl)-5-[4-(4-morpholinyl)phenyl]-2-pyrazoline (**2g**).* Pale yellow powder. Yield: 88%. Mp 162−164 °C. IR ν_{max} (cm^{-1}): 3091.89, 3032.10, 2966.52, 2910.58, 2895.15, 2854.65, 2831.50, 1608.63, 1595.13, 1517.98, 1490.97, 1448.54, 1423.47, 1381.03, 1365.60, 1334.74, 1307.74, 1301.95, 1284.59, 1244.09, 1211.30, 1192.01, 1172.72, 1122.57, 1093.64, 1072.42, 1053.13, 1020.34, 1008.77, 991.41, 923.90, 885.33, 873.75, 842.89, 812.03, 771.53, 731.02, 709.80, 688.59, 642.30, 623.01, 572.86, 553.57, 532.35. ^{1}H NMR (500 MHz, DMSO-d_6) δ (ppm): 3.03−3.08 (m, 5H), 3.70 (t, J = 4.60, 4.95 Hz, 4H), 3.83 (dd, J_{BA} = 17.45 Hz, J_{BX} = 12.00 Hz, 1H), 5.35 (dd, J_{BX} = 11.85 Hz, J_{AX} = 5.70 Hz, 1H), 6.89 (d, J = 8.80 Hz, 2H), 6.97 (d, J = 9.05 Hz, 2H), 7.10 (d, J = 8.70 Hz, 2H), 7.17 (d, J = 9.05 Hz, 2H), 7.58 (dd, J = 1.15, 5.05 Hz, 1H), 7.63−7.65 (m, 1H), 7.72−7.73 (m, 1H). ^{13}C NMR (125 MHz, DMSO-d_6) δ (ppm): 44.42 (CH_2), 48.71 ($2CH_2$), 62.73 (CH), 66.54 ($2CH_2$), 114.75 (2CH), 115.89 (2CH), 122.21 (CH), 125.14 (CH), 125.67 (CH), 127.01 (2CH), 127.86 (C), 129.04 (2CH), 132.76 (C), 135.08 (C), 143.66 (C), 145.68 (C), 150.78 (C). HRMS (m/z): $[M + H]^+$ calcd for $C_{23}H_{22}ClN_3OS$: 424.1245. Found: 424.1237.

*4.2.2.8. 1-(4-Bromophenyl)-3-(thiophen-3-yl)-5-[4-(4-morpholinyl)phenyl]-2-pyrazoline (**2h**).* Light yellow powder. Yield: 82%. Mp 175−177 °C. IR ν_{max} (cm^{-1}): 3099.61, 2960.73, 2916.37, 2893.22, 2858.51, 2821.86, 1612.49, 1591.27, 1556.55, 1514.12, 1489.05, 1444.68, 1423.47, 1377.17, 1359.82, 1334.74, 1307.74, 1259.52, 1234.44, 1213.23, 1190.08, 1178.51, 1120.64, 1087.85, 1072.42, 1051.20, 1026.13, 1001.06, 926.69, 864.11, 842.89, 808.17, 800.46, 771.53, 729.09, 702.09, 636.51, 623.01, 574.79, 543.93. ^{1}H NMR (500 MHz, DMSO-d_6) δ (ppm): 3.05−3.08 (m, 5H), 3.70 (t, J = 4.60, 5.00 Hz, 4H), 3.83 (dd, J_{BA} = 17.40 Hz, J_{BX} = 11.95 Hz, 1H), 5.35 (dd, J_{BX} = 11.85 Hz, J_{AX} = 5.60 Hz, 1H), 6.88 (d, J = 8.80 Hz, 2H), 6.92 (d, J = 9.05 Hz, 2H), 7.09 (d, J = 8.75 Hz, 2H), 7.28 (d, J = 9.05 Hz, 2H), 7.57 (dd, J = 1.15, 5.05 Hz, 1H), 7.63−7.65 (m, 1H), 7.73−7.74 (m, 1H). ^{13}C NMR (125 MHz, DMSO-d_6) δ (ppm): 44.41 (CH_2), 48.71 ($2CH_2$), 62.62 (CH), 66.54 ($2CH_2$), 109.82 (C), 115.26 (2CH), 115.89 (2CH), 125.19 (CH), 125.67 (CH), 126.99 (2CH), 127.87 (CH), 131.87 (2CH), 132.69 (C), 135.06 (C), 143.96 (C), 145.76 (C), 150.78 (C). HRMS (m/z): $[M + H]^+$ calcd for $C_{23}H_{22}BrN_3OS$: 468.0740. Found: 468.0751.

*4.2.2.9. 1-(3-Fluorophenyl)-3-(thiophen-3-yl)-5-[4-(4-morpholinyl)phenyl]-2-pyrazoline (**2i**).* Light yellow-green powder. Yield: 48%. Mp 142−144 °C. IR ν_{max} (cm^{-1}): 3086.11, 3070.68, 3035.96, 2962.66, 2916.37, 2891.30, 2873.94, 2848.86, 2833.43, 1612.49, 1577.77, 1516.05, 1489.05, 1448.54, 1425.40, 1381.03, 1346.31, 1303.88, 1284.59, 1263.37, 1234.44, 1209.37, 1176.51, 1153.43, 1120.64, 1083.99, 1064.71, 1049.28, 1031.92, 1012.63, 960.55, 933.55, 925.83, 891.11, 869.90, 824.89, 821.68, 798.53, 756.10, 729.09, 678.94, 659.66, 626.87, 576.72, 549.71. ^{1}H NMR (500 MHz, DMSO-d_6) δ (ppm): 3.05−3.09 (m, 5H), 3.70 (t, J = 4.60, 4.95 Hz, 4H), 3.84 (dd, J_{BA} = 17.45 Hz, J_{BX} = 12.00 Hz, 1H), 5.37 (dd, J_{BX} = 11.90 Hz, J_{AX} = 5.65 Hz, 1H), 6.45−6.49 (m, 1H), 6.73−6.79 (m, 2H), 6.90

https://doi.org/10.1021/acsomega.3c10490
ACS Omega 2024, 9, 31401−31409

(d, J = 8.80 Hz, 2H), 7.11−7.16 (m, 3H), 7.60 (dd, J = 1.10, 6.15 Hz, 1H), 7.64−7.66 (m, 1H), 7.75−7.76 (m, 1H). ^{13}C NMR (125 MHz, DMSO-d_6) δ (ppm): 44.41 (CH_2), 48.70 ($2CH_2$), 62.66 (CH), 66.54 ($2CH_2$), 99.94 (CH), 100.16 (CH), 104.77 (CH, d, J = 21.25 Hz), 109.25 (CH), 115.90 (2CH), 125.37 (CH), 125.76 (CH), 126.99 (2CH), 127.86 (CH), 130.84 (C, d, J = 10.06 Hz), 132.83 and 135.00 (C), 145.99 (C), 146.49 (C, d, J = 11.00 Hz), 150.80 (C), 162.43 and 164.33 (C). HRMS (m/z): $[M + H]^+$ calcd for $C_{23}H_{22}FN_3OS$: 408.1540. Found: 408.1538.

*4.2.2.10. 1-(3-Chlorophenyl)-3-(thiophen-3-yl)-5-[4-(4-morpholinyl)phenyl]-2-pyrazoline (**2j**).* Pale yellow powder. Yield: 94%. Mp 159−161 °C. IR ν_{max} (cm^{-1}): 3115.04, 3097.68, 3030.17, 2956.87, 2862.36, 2831.50, 1612.49, 1589.34, 1560.41, 1539.20, 1514.12, 1483.26, 1446.61, 1427.32, 1379.10, 1354.03, 1303.88, 1261.45, 1234.44, 1209.37, 1190.08, 1157.29, 1120.64, 1112.93, 1083.99, 1053.13, 1024.20, 1010.70, 999.13, 985.62, 925.83, 877.61, 844.82, 825.53, 798.53, 775.38, 740.67, 731.02, 680.87, 636.51, 624.94, 582.50, 569.00, 543.93. ^{1}H NMR (500 MHz, DMSO-d_6) δ (ppm): 3.04−3.09 (m, 5H), 3.70 (t, J = 4.60, 5.00 Hz, 4H), 3.83 (dd, J_{BA} = 17.50 Hz, J_{BX} = 12.00 Hz, 1H), 5.38 (dd, J_{BX} = 11.85 Hz, J_{AX} = 5.50 Hz, 1H), 6.69−6.71 (m, 1H), 6.83−6.85 (m, 1H), 6.89 (d, J = 8.80 Hz, 2H), 7.05 (t, J = 2.05, 2.10 Hz, 1H), 7.10−7.14 (m, 3H), 7.60 (dd, J = 1.20, 5.05 Hz, 1H), 7.64−7.65 (m, 1H), 7.75−7.76 (m, 1H). ^{13}C NMR (125 MHz, DMSO-d_6) δ (ppm): 44.40 (CH_2), 48.67 ($2CH_2$), 62.50 (CH), 66.54 ($2CH_2$), 111.76 (CH), 112.68 (CH), 115.89 (2CH), 118.02 (CH), 125.46 (CH), 125.78 (CH), 126.97 (2CH), 127.87 (CH), 130.86 (CH), 132.67 (C), 133.98 (C), 134.95 (C), 145.97 (C), 146.18 (C), 150.80 (C). HRMS (m/z): $[M + H]^+$ calcd for $C_{23}H_{22}ClN_3OS$: 424.1245. Found: 424.1243.

*4.2.2.11. 1-(3-Bromophenyl)-3-(thiophen-3-yl)-5-[4-(4-morpholinyl)phenyl]-2-pyrazoline (**2k**).* Pale yellow powder. Yield: 62%. Mp 152−153 °C. IR ν_{max} (cm^{-1}): 3111.18, 3095.75, 3030.17, 2985.81, 2956.87, 2918.30, 2860.43, 2833.43, 1610.56, 1585.49, 1552.70, 1514.12, 1481.33, 1446.61, 1423.47, 1390.68, 1379.10, 1354.03, 1303.88, 1259.52, 1234.44, 1209.37, 1188.15, 1174.65, 1120.64, 1112.93, 1074.35, 1051.20, 1022.27, 1008.77, 997.20, 983.70, 925.83, 877.61, 842.89, 825.53, 798.53, 773.46, 721.38, 678.94, 636.51, 624.94, 582.50, 557.43, 543.93. ^{1}H NMR (500 MHz, DMSO-d_6) δ (ppm): 3.06−3.09 (m, 5H), 3.70 (t, J = 4.60, 4.95 Hz, 4H), 3.84 (dd, J_{BA} = 17.45 Hz, J_{BX} = 11.95 Hz, 1H), 5.38 (dd, J_{BX} = 11.85 Hz, J_{AX} = 5.45 Hz, 1H), 6.82−6.90 (m, 4H), 7.06 (t, J = 8.05, 8.10 Hz, 1H), 7.11 (d, J = 8.75 Hz, 2H), 7.21 (t, J = 1.95, 2.00 Hz, 1H), 7.60 (dd, J = 1.15, 5.05 Hz, 1H), 7.64−7.65 (m, 1H), 7.76−7.77 (m, 1H). ^{13}C NMR (125 MHz, DMSO-d_6) δ (ppm): 44.39 (CH_2), 48.67 ($2CH_2$), 62.46 (CH), 66.54 ($2CH_2$), 112.09 (CH), 115.52 (CH), 115.89 (2CH), 120.89 (CH), 122.65 (CH), 125.48 (CH), 125.79 (CH), 126.98 (2CH), 127.88 (CH), 131.15 (C), 132.64 (C), 134.94 (C), 146.08 (C), 146.22 (C), 150.80 (C). HRMS (m/z): $[M + H]^+$ calcd for $C_{23}H_{22}BrN_3OS$: 468.0740. Found: 468.0739.

*4.2.2.12. 1-(3-Nitrophenyl)-3-(thiophen-3-yl)-5-[4-(4-morpholinyl)phenyl]-2-pyrazoline (**2l**).* Mustard-colored powder. Yield: 70%. Mp 125−127 °C. IR ν_{max} (cm^{-1}): 3103.48, 3032.10, 2964.59, 2918.30, 2848.86, 1612.49, 1585.49, 1568.13, 1527.62, 1487.12, 1444.68, 1423.47, 1363.67, 1342.46, 1307.74, 1280.73, 1259.52, 1234.44, 1192.01, 1172.72, 1155.36, 1120.64, 1111.00, 1089.78, 1066.64, 1051.20, 1026.13, 1014.56, 987.55, 925.83, 877.61, 864.11, 848.68, 839.03, 817.82, 786.96, 775.38, 727.16, 669.30, 653.87, 634.58, 617.22, 580.57, 553.57. ^{1}H NMR (500 MHz, DMSO-d_6) δ (ppm): 3.05 (t, J = 4.65, 5.00 Hz, 4H), 3.14 (dd, J_{AB} = 17.55 Hz, J_{AX} = 5.45 Hz, 1H), 3.69 (t, J = 4.50, 5.00 Hz, 4H), 3.90 (dd, J_{BA} = 17.50 Hz, J_{BX} = 11.85 Hz, 1H), 5.49 (dd, J_{BX} = 11.80 Hz, J_{AX} = 5.35 Hz, 1H), 6.90 (d, J = 8.75 Hz, 2H), 7.14 (d, J = 8.70 Hz, 2H), 7.27−7.29 (m, 1H), 7.40 (t, J = 8.15, 8.20 Hz, 1H), 7.49−7.51 (m, 1H), 7.62−7.68 (m, 2H), 7.80−7.83 (m, 2H). ^{13}C NMR (125 MHz, DMSO-d_6) δ (ppm): 44.53 (CH_2), 48.61 ($2CH_2$), 62.51 (CH), 66.51 ($2CH_2$), 106.98 (CH), 112.66 (CH), 115.92 (2CH), 119.09 (CH), 125.78 (CH), 126.10 (CH), 127.06 (2CH), 128.04 (CH), 130.60 (CH), 132.07 (C), 134.67 (C), 145.40 (C), 147.24 (C), 148.99 (C), 150.88 (C). HRMS (m/z): $[M + H]^+$ calcd for $C_{23}H_{22}N_4O_3S$: 435.1485. Found: 435.1488.

4.3. *In Vitro* Assay for AChE and BuChE Inhibition. Human AChE (CAS No: 9000-81-1) and human BuChE (CAS No: 9001-08-5), 5,5′-dithiobis(2-nitrobenzoic acide) (DTNB), tacrine, and donepezil hydrochloride were purchased from Sigma-Aldrich (Steinheim, Germany). Acetylthiocholine iodide (ATC) and butyrylthiocholine iodide (BTC) were obtained from Fluka (Germany). All pipetting processes were performed using a Biotek Precision XS robotic system (USA). Measurements of the percentage inhibition were carried out at 412 nm by using a BioTek-Synergy H1 microplate reader (USA). The inhibitory activities of the compounds against AChE and BChE were determined in 96-well plates by a modified spectrophotometric method[38−42] reported by Ellman et al.[32] using donepezil and tacrine as reference drugs. Initially, the synthesized compounds **1** and **2a−l** were prepared at two concentrations (10^{-3} and 10^{-4} M) using 2% DMSO, and inhibition potencies were measured. Then, the selected compounds (**2a**, **2g**, **2j**, **2l**) displaying more than 50% inhibition were tested at further concentrations (10^{-5}−10^{-9} M).

The final volume of a well was 210 μL consisting of 140 μL phosphate buffer (0.1 M, pH = 8), 20 μL inhibitor solution, 20 μL enzyme solution (2.5 U/mL), 20 μL DTNB (0.01 M), and 10 μL substrate solution (0.075 M ATC or BTC). First of all, the solutions of inhibitor, enzyme, and DTNB were added to phosphate buffer and incubated at 25 °C for 15 min. After the incubation, the substrate (ATC or BTC) was added to the enzyme−inhibitor mixture. The production of the yellow anion (5-thio-2-nitrobenzoic acid) was recorded for 5 min at 412 nm. As a control, an identical solution of the enzyme without the inhibitor was processed. Control and inhibitor readings were corrected with blank readings. Each concentration was analyzed in quadruplicate. The IC_{50} values were calculated from a dose−response curve obtained by plotting the percentage inhibition versus the log concentration with the use of GraphPad "PRISM" software (version 6.0). The results were displayed as mean ± standard deviation (SD).

4.4. *In Vitro* BBB Permeability Assay. To observe the BBB crossing ability of the most active compounds (**2a**, **2g**, **2j**, and **2l**), the PAMPA was performed, as previously described.[43,44]

4.5. Molecular Docking Studies. Compounds **2a**, **2g**, **2j**, and **2l**, which were determined as promising inhibitors of AChE, were subjected to *in silico* docking using the structure-based approach to identify the potential binding and the interaction locations at the AChE active site. In order to conduct *in silico* studies, protein−ligand interaction analysis

https://doi.org/10.1021/acsomega.3c10490
ACS Omega 2024, 9, 31401−31409

was performed utilizing the crystal structure of the AChE (PDB: 4EY7)[33] by using the Schrödinger Suite 2020 -Maestro interface as mentioned in the previous studies.[38−42] The crystal structure was first prepared for docking studies with the Protein Preparation Wizard protocol in Schrödinger Suite 2020, the bond lengths were adjusted using the OPLS 2005 force field, and the possible charges of the atoms on the charged amino acids under the specified ambient conditions were determined automatically. The compounds were prepared for molecular docking studies using the Ligprep 3.8 module.[45] Grids were generated with Glide 7.1[46] and docking runs were performed with the single precision docking mode of the same module.

■ ASSOCIATED CONTENT

Supporting Information

The Supporting Information is available free of charge at https://pubs.acs.org/doi/10.1021/acsomega.3c10490.

IR, ^{1}H NMR, ^{13}C NMR, and HRMS spectra of compounds **1**, **2a−l** (PDF)

■ AUTHOR INFORMATION

Corresponding Author

Ahmet Özdemir − *Department of Pharmaceutical Chemistry, Faculty of Pharmacy, Anadolu University, 26470 Eskişehir, Turkey;* orcid.org/0000-0003-0280-5550; Email: ahmeto@anadolu.edu.tr

Authors

Mehlika Dilek Altıntop − *Department of Pharmaceutical Chemistry, Faculty of Pharmacy, Anadolu University, 26470 Eskişehir, Turkey;* orcid.org/0000-0002-8159-663X

Begüm Nurpelin Sağlık Özkan − *Department of Pharmaceutical Chemistry, Faculty of Pharmacy, Anadolu University, 26470 Eskişehir, Turkey;* orcid.org/0000-0002-0151-6266

Complete contact information is available at: https://pubs.acs.org/10.1021/acsomega.3c10490

Author Contributions

M.D.A. and A.Ö. designed the research and performed the preparation and characterization of all compounds; B.N.S.Ö. fulfilled *in vitro* experimental studies as well as *in silico* studies. M.D.A. and A.Ö. mainly wrote the manuscript. A.Ö. was responsible for the correspondence of the manuscript. All authors discussed, edited, and approved the final version of the manuscript.

Notes

The authors declare no competing financial interest.

■ ACKNOWLEDGMENTS

This study was supported by Anadolu University Scientific Research Projects Commission under the grant no 2207S114.

■ REFERENCES

(1) Monteiro, A. R.; Barbosa, D. J.; Remião, F.; Silva, R. Alzheimer's disease: Insights and new prospects in disease pathophysiology, biomarkers and disease-modifying drugs. *Biochem. Pharmacol.* **2023**, *211*, 115522.

(2) Khan, S. S.; Khatik, G. L.; Datusalia, A. K. Strategies for treatment of disease-associated dementia beyond Alzheimer's Disease: An update. *Curr. Neuropharmacol.* **2023**, *21* (2), 309−339.

(3) Patel, A.; Shah, D.; Patel, Y.; Patel, S.; Mehta, M.; Bambharoliya, T. A review on recent development of novel heterocycles as acetylcholinesterase inhibitor for the treatment of Alzheimer's Disease. *Curr. Drug Targets* **2023**, *24* (3), 225−246.

(4) Maurer, S. V.; Williams, C. L. The cholinergic system modulates memory and hippocampal plasticity via its interactions with non-neuronal cells. *Front. Immunol.* **2017**, *8*, 1489.

(5) Sarabia-Vallejo, Á.; López-Alvarado, P.; Menéndez, J. C. Small-molecule theranostics in Alzheimer's disease. *Eur. J. Med. Chem.* **2023**, *255*, 115382.

(6) Al-Ghraiybah, N. F.; Wang, J.; Alkhalifa, A. E.; Roberts, A. B.; Raj, R.; Yang, E.; Kaddoumi, A. Glial cell-mediated neuroinflammation in Alzheimer's Disease. *Int. J. Mol. Sci.* **2022**, *23* (18), 10572.

(7) Godyń, J.; Jończyk, J.; Panek, D.; Malawska, B. Therapeutic strategies for Alzheimer's disease in clinical trials. *Pharmacol. Rep.* **2016**, *68* (1), 127−138.

(8) Self, W. K.; Holtzman, D. M. Emerging diagnostics and therapeutics for Alzheimer disease. *Nat. Med.* **2023**, *29*, 2187−2199.

(9) Sang, Z.; Wang, K.; Dong, J.; Tang, L. Alzheimer's disease: Updated multi-targets therapeutics are in clinical and in progress. *Eur. J. Med. Chem.* **2022**, *238*, 114464.

(10) Passeri, E.; Elkhoury, K.; Morsink, M.; Broersen, K.; Linder, M.; Tamayol, A.; Malaplate, C.; Yen, F. T.; Arab-Tehrany, E. Alzheimer's Disease: Treatment strategies and their limitations. *Int. J. Mol. Sci.* **2022**, *23* (22), 13954.

(11) Se Thoe, E.; Fauzi, A.; Tang, Y. Q.; Chamyuang, S.; Chia, A. Y. Y. A review on advances of treatment modalities for Alzheimer's disease. *Life Sci.* **2021**, *276*, No. 119129.

(12) Nehra, B.; Rulhania, S.; Jaswal, S.; Kumar, B.; Singh, G.; Monga, V. Recent advancements in the development of bioactive pyrazoline derivatives. *Eur. J. Med. Chem.* **2020**, *205*, 112666.

(13) Abou-Zied, H. A.; Beshr, E. A. M.; Hayallah, A. M.; Abdel-Aziz, M. Emerging insights into pyrazoline motifs: A comprehensive exploration of biological mechanisms and prospects for future advancements. *J. Mol. Struct.* **2024**, *1296*, 136807.

(14) Kumar, A.; Nehra, B.; Singh, D.; Kumar, D.; Chawla, P. A. Recent advances in the development of nitrogen-containing heterocyclic anti-alzheimer's agents. *Curr. Top. Med. Chem.* **2023**, *23* (13), 1277−1306.

(15) Ahsan, M. J.; Ali, A.; Ali, A.; Thiriveedhi, A.; Bakht, M. A.; Yusuf, M.; Salahuddin Afzal, O.; Altamimi, A. S. A. Pyrazoline containing compounds as therapeutic targets for neurodegenerative disorders. *ACS Omega* **2022**, *7* (43), 38207−38245.

(16) Mantzanidou, M.; Pontiki, E.; Hadjipavlou-Litina, D. Pyrazoles and pyrazolines as anti-inflammatory agents. *Molecules* **2021**, *26* (11), 3439.

(17) Mathew, B.; Parambi, D. G. T.; Mathew, G. E.; Uddin, M. S.; Inasu, S. T.; Kim, H.; Marathakam, A.; Unnikrishnan, M. K.; Carradori, S. Emerging therapeutic potentials of dual-acting MAO and AChE inhibitors in Alzheimer's and Parkinson's diseases. *Arch. Pharm.* **2019**, *352* (11), No. e1900177.

(18) Alex, J. M.; Kumar, R. 4,5-Dihydro-1*H*-pyrazole: An indispensable scaffold. *J. Enzyme Inhib. Med. Chem.* **2014**, *29* (3), 427−442.

(19) Shaaban, M. R.; Mayhoub, A. S.; Farag, A. M. Recent advances in the therapeutic applications of pyrazolines. *Expert Opin. Ther. Pat.* **2012**, *22* (3), 253−291.

(20) Machado, V.; Cenci, A. R.; Teixeira, K. F.; Sens, L.; Tizziani, T.; Nunes, R. J.; Ferreira, L. L. G.; Yunes, R. A.; Sandjo, L. P.; Andricopulo, A. D.; de Oliveira, A. S. Pyrazolines as potential anti-Alzheimer's agents: DFT, molecular docking, enzyme inhibition and pharmacokinetic studies. *RSC Med. Chem.* **2022**, *13* (12), 1644−1656.

(21) Yamali, C.; Gul, H. I.; Kazaz, C.; Levent, S.; Gulcin, I. Synthesis, structure elucidation, and *in vitro* pharmacological evaluation of novel polyfluoro substituted pyrazoline type sulfonamides as multi-target agents for inhibition of acetylcholinesterase and carbonic anhydrase I and II enzymes. *Bioorg. Chem.* **2020**, *96*, 103627.

(22) Ozmen Ozgun, D.; Gul, H. I.; Yamali, C.; Sakagami, H.; Gulcin, I.; Sukuroglu, M.; Supuran, C. T. Synthesis and bioactivities of pyrazoline benzensulfonamides as carbonic anhydrase and acetylcholinesterase inhibitors with low cytotoxicity. *Bioorg. Chem.* **2019**, *84*, 511−517.
(23) Unsal-Tan, O.; Tüylü Küçükkılınç, T.; Ayazgök, B.; Balkan, A.; Ozadali-Sari, K. Synthesis, molecular docking, and biological evaluation of novel 2-pyrazoline derivatives as multifunctional agents for the treatment of Alzheimer's disease. *Medchemcomm.* **2019**, *10* (6), 1018−1026.
(24) Altintop, M. D.; Özdemir, A.; Kaplancikli, Z. A.; Turan-Zitouni, G.; Temel, H. E.; Çiftçi, G. A. Synthesis and biological evaluation of some pyrazoline derivatives bearing a dithiocarbamate moiety as new cholinesterase inhibitors. *Arch. Pharm.* **2013**, *346*, 189−199.
(25) Altıntop, M. D. Synthesis, *in vitro* and *in silico* evaluation of a series of pyrazolines as new anticholinesterase agents. *Lett. Drug Des. Discovery* **2020**, *17*, 574−584.
(26) Temel, H. E.; Altıntop, M. D.; Özdemir, A. Synthesis and evaluation of a new series of thiazolyl-pyrazoline derivatives as cholinesterase inhibitors. *Turk. J. Pharm. Sci.* **2018**, *15* (3), 333−338.
(27) Chawla, S.; Sharma, S.; Kashid, S.; Verma, P. K.; Sapra, A. Therapeutic potential of thiophene compounds: A mini-review. *Mini-Rev. Med. Chem.* **2023**, *23* (15), 1514−1534.
(28) Gramec, D.; Peterlin Mašič, L.; Sollner Dolenc, M. Bioactivation potential of thiophene-containing drugs. *Chem. Res. Toxicol.* **2014**, *27* (8), 1344−1358.
(29) Hasan, A. H.; Murugesan, S.; Amran, S. I.; Chander, S.; Alanazi, M. M.; Hadda, T. B.; Shakya, S.; Pratama, M. R. F.; Das, B.; Biswas, S.; Jamalis, J. Novel thiophene chalcones-coumarin as acetylcholinesterase inhibitors: Design, synthesis, biological evaluation, molecular docking, ADMET prediction and molecular dynamics simulation. *Bioorg. Chem.* **2022**, *119*, 105572.
(30) Cetin, A.; Türkan, F.; Taslimi, P.; Gulçin, İ. Synthesis and characterization of novel substituted thiophene derivatives and discovery of their carbonic anhydrase and acetylcholinesterase inhibition effects. *J. Biochem. Mol. Toxicol.* **2019**, *33* (3), No. e22261.
(31) Shah, M. S.; Khan, S. U.; Ejaz, S. A.; Afridi, S.; Rizvi, S. U. F.; Najam-Ul-Haq, M.; Iqbal, J. Cholinesterases inhibition and molecular modeling studies of piperidyl-thienyl and 2-pyrazoline derivatives of chalcones. *Biochem. Biophys. Res. Commun.* **2017**, *482* (4), 615−624.
(32) Ellman, G. L.; Courtney, K. D.; Andres, V.; Feather-Stone, R. M. A new and rapid colorimetric determination of acetylcholinesterase activity. *Biochem. Pharmacol.* **1961**, *7*, 88−95.
(33) Cheung, J.; Rudolph, M. J.; Burshteyn, F.; Cassidy, M. S.; Gary, E. N.; Love, J.; Franklin, M. C.; Height, J. J. Structures of human acetylcholinesterase in complex with pharmacologically important ligands. *J. Med. Chem.* **2012**, *55*, 10282−10286.
(34) Altıntop, M. D.; Cantürk, Z.; Özdemir, A. Design, synthesis, and evaluation of a new series of 2-pyrazolines as potential antileukemic agents. *ACS Omega.* **2023**, *8* (45), 42867−42877.
(35) Özdemir, A.; Turan-Zitouni, G.; Kaplancikli, Z. A.; Revial, G.; Guven, K. Synthesis and antimicrobial activity of 1-(4-aryl-2-thiazolyl)-3-(2-thienyl)-5-aryl-2-pyrazoline derivatives. *Eur. J. Med. Chem.* **2007**, *42* (2), 403−409.
(36) Özdemir, A.; Altıntop, M. D.; Kaplancıklı, Z. A.; Can, Ö. D.; Demir Özkay, Ü.; Turan-Zitouni, G. Synthesis and evaluation of new 1,5-diaryl-3-[4-(methylsulfonyl)phenyl]-4,5-dihydro-1*H*-pyrazole derivatives as potential antidepressant agents. *Molecules* **2015**, *20*, 2668−2684.
(37) Özdemir, A.; Altıntop, M. D.; Kaplancıklı, Z. A.; Turan-Zitouni, G.; Akalın Ciftçi, G.; Demirci, F. Synthesis and biological evaluation of a new series of pyrazolines as new anticandidal agents. *Pharm. Chem. J.* **2014**, *48*, 603−612.
(38) Maestro. *Version 2020, 10.6*; Schrödinger, LLC: New York, NY, USA.
(39) Sağlık, B. N.; Levent, S.; Osmaniye, D.; Evren, A. E.; Karaduman, A. B.; Özkay, Y.; Kaplancıklı, Z. A. Design, synthesis, and *in vitro* and *in silico* approaches of novel indanone derivatives as multifunctional anti-Alzheimer agents. *ACS Omega* **2022**, *7* (50), 47378−47404.
(40) Osmaniye, D.; Evren, A. E.; Sağlık, B. N.; Levent, S.; Özkay, Y.; Kaplancıklı, Z. A. Design, synthesis, biological activity, molecular docking, and molecular dynamics of novel benzimidazole derivatives as potential AChE/MAO-B dual inhibitors. *Arch. Pharm.* **2022**, *355* (3), No. e2100450.
(41) Tok, F.; Kocyigit-Kaymakcioglu, B.; Saglik, B. N.; Levent, S.; Ozkay, Y.; Kaplancikli, Z. A. Synthesis and biological evaluation of new pyrazolone Schiff bases as monoamine oxidase and cholinesterase inhibitors. *Bioorg. Chem.* **2019**, *84*, 41−50.
(42) Sağlık, B. N.; Ilgın, S.; Özkay, Y. Synthesis of new donepezil analogues and investigation of their effects on cholinesterase enzymes. *Eur. J. Med. Chem.* **2016**, *124*, 1026−1040.
(43) Sağlık, B. N.; Osmaniye, D.; Acar Çevik, U.; Levent, S.; Kaya Çavuşoğlu, B.; Özkay, Y.; Kaplancıklı, Z. A. Design, synthesis, and structure-activity relationships of thiazole analogs as anticholinesterase agents for Alzheimer's Disease. *Molecules* **2020**, *25* (18), 4312.
(44) Yan, G.; Hao, L.; Niu, Y.; Huang, W.; Wang, W.; Xu, F.; Liang, L.; Wang, C.; Jin, H.; Xu, P. 2-Substituted-thio- *N*-(4-substituted-thiazol/1*H*-imidazol-2-yl)acetamides as BACE1 inhibitors: Synthesis, biological evaluation and docking studies. *Eur. J. Med. Chem.* **2017**, *137*, 462−475.
(45) LigPrep, Version 3.8, L. Schrödinger, Schrödinger, LLC: New York, NY, USA.
(46) Glide, Version 7.1, L. Schrödinger, Schrödinger, LLC: New York, NY, USA.

https://doi.org/10.1021/acsomega.3c10490
ACS Omega 2024, 9, 31401−31409